Bio-Design and Manufacturing (2023) 6:284–297
https://doi.org/10.1007/s42242-022-00227-x

RESEARCH ARTICLE

Gelatin-based hydrogel functionalized with taurine moieties for in vivo skin tissue regeneration

Farnaz Rahimi[1] · Nima Ahmadkhani[2] · Aida Goodarzi[1] · Fariba Noori[1] · Sajad Hassanzadeh[3,4] · Sepideh Saghati[5] · Mehdi Khanmohammadi[4] · Arash Goodarzi[1]

Received: 11 July 2022 / Accepted: 15 December 2022 / Published online: 28 March 2023

Abstract

Functionalized hydrogels stimulate the migration and morphogenesis of endothelial cells (ECs) and are useful substrates for wound healing. The present study investigates the feasibility of covalent conjugation of taurine (Tau) on a gelatin-based hydrogel. This hydrogel is expected to maintain positive charged growth factors such as basic fibroblast growth factor (bFGF) and vascular endothelial growth factors (VEGFs) near ECs within the hydrogel microenvironment. The gelatin was conjugated with hydroxyl phenol (Ph) and Tau moieties, and in following that Ph residues were crosslinked through a horseradish peroxidase-catalyzed reaction. The migration characteristics of ECs were analyzed by scratch migration assay and microparticle-based cell migration assay. Cellular morphology and amounts of angiopoietin 1 (Ang 1), bFGF, and VEGF proteins were evaluated for encapsulated cells. The potential of synthesized hydrogels in wound healing was assessed by the percentage of reduction from the original wound size and histopathological analyses of rat skin. The incorporated Tau molecules within the hydrogel remained stable through covalent bonds during incubation. During extended incubation, the gelatin-based hydrogel conjugated with Tau improved the migration distance and number of existing migrated ECs. Immobilized Tau within the gelatin-based hydrogel induced high motility of ECs, accompanied by robust cytoskeleton extension and a cell subpopulation that expressed CD44 and CD31 receptors as well as enhancement of Ang 1, bFGF, and VEGF. We found that injectable Gel-Ph-Tau effectively improves wound-healing parameters.

✉ Mehdi Khanmohammadi
Mehdi.khanmohammadi84@gmail.com;
khanmohammadi.mehdi@iums.ac.ir

✉ Arash Goodarzi
dvm.goodarzi86@yahoo.com

1 Department of Tissue Engineering, School of Advanced Technologies in Medicine, Fasa University of Medical Science, Fasa, Iran

2 School of Chemical, Biological and Environmental Engineering, Oregon State University, Corvallis, OR 97331, USA

3 Eye Research Center, School of Medicine, The Five Senses Health Institute, Iran University of Medical Sciences, Tehran, Iran

4 Skull Base Research Center, School of Medicine, The Five Senses Health Institute, Iran University of Medical Sciences, Tehran, Iran

5 Department of Tissue Engineering, Faculty of Advanced Medical Sciences, Tabriz University of Medical Sciences, Tabriz, Iran

Graphic abstract

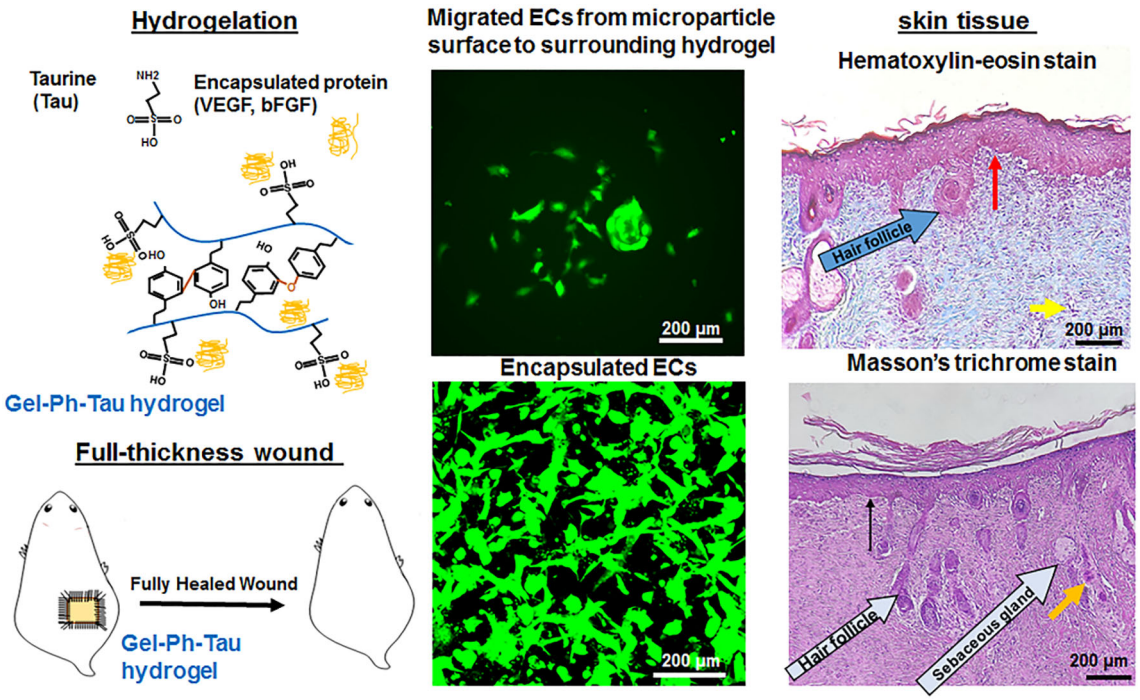

Keywords Taurine conjugation · Covalent crosslinking · Immobilization of growth factors · Gelatin-based hydrogel · Endothelial cells

Introduction

Treatment of skin wounds is one of the most expensive global healthcare challenges [1, 2]. In addition, wound healing can be fragile and may lead to chronic, incurable wounds that rupture or fail. Issues involved in chronic wound healing include diabetes, venous or arterial disease, infection, and metabolic deficiencies in old age [3, 4]. The wound-healing process is a pathological condition affecting the anatomical and functional structure of the skin. Inflammation, proliferation, migration, and remodeling are the four phases of wound healing [4–6]. Immediately after injury, hemostasis occurs, and involves platelet aggregation and blood coagulation. In the second phase, neutrophils and reactive oxygen species (ROS) clean debris and eliminate bacteria [7]. The proliferation phase is accompanied by an accumulation of numerous skin cells and formation of granulation tissue. In this phase, extracellular matrix (ECM) components (collagen, hyaluronic acid, proteoglycans, and elastin) play a significant role in the granulation process. Formation of new tissue is also influenced by growth factors and cytokines [8, 9]. Finally, in the remodeling phase, fibroblasts cover the entire injury [10].

As noted, ECM plays an important role in wound healing; therefore, replicating its features with materials can be helpful. Hydrogels are three-dimensional (3D), hydrophilic, highly absorbent cross-linked polymer networks, and capable of absorbing a great quantity of water or biological fluids. They have a soft network consistency similar to that of native ECM [11–13]. In other words, hydrogels more closely resemble natural living tissue environments than other scaffold types, making them promising scaffold materials for many tissue engineering and regenerative medicine applications [14]. Selection of suitable hydrogel materials and availability of biofunctional groups, and finding the best methods of manufacturing matrices with desirable characteristics, are vital factors in tissue regeneration research [15, 16]. Several natural and synthetic hydrogels functionalized with bioactive groups have been employed as wound dressing substrates [17–19]. Natural hydrogels such as hyaluronic acid [20], fibrin [21], and collagen [22] and its denatured form gelatin [23], contain bioactive and/or cell adhesive sequences that provide cell attachment, proliferation, and migration. However, promotion of hydrogel bioactivity and function through immobilization of such molecules in the hydrogel structure would upregulate their effectiveness in

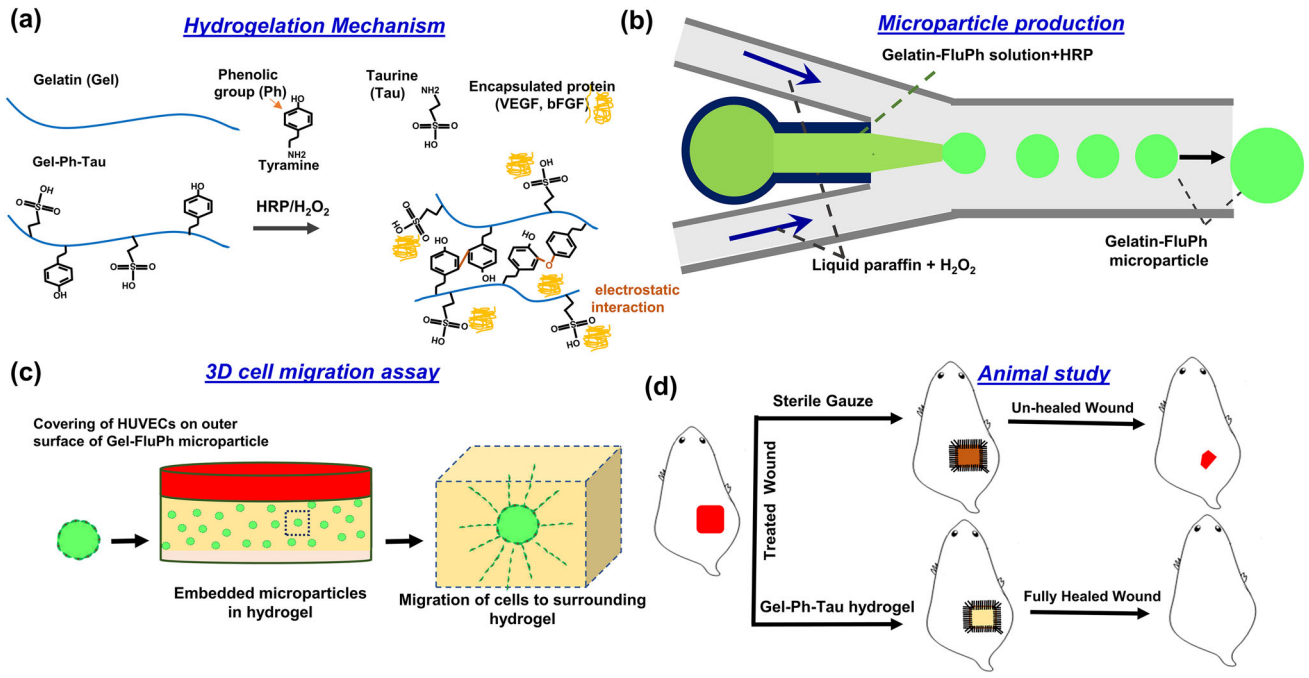

Fig. 1 **a** Schematic illustrations of a conjugated phenol (Ph) group and taurine (Tau) on gelatin backbone, and hydrogel formation through horseradish peroxidase (HRP) catalyzed crosslinks between Ph moieties in Gel-Ph-Tau. **b** Gel-FluPh microparticle production through the microfluidic system. **c** Covered microparticles with layer of endothelial cells (ECs), and embedding in gelatin-based hydrogel for the microparticle-based cell migration assay. **d** Wound-healing study

biomedical applications [24]. The novel properties of gelatin have attracted a great deal of attention. Gelatin has excellent features, such as hemostatic properties, biocompatibility, non-toxicity, low antigenicity, non-immunogenicity, and cell binding sites, making it suitable for biomedical applications [25, 26]. Functional groups in gelatin allow it to be modified and crosslinked with different crosslinking techniques (chemical and enzymatic) for hydrogel formation [24, 25, 27, 28]. The hydrogelation via peroxidase-catalyzation due to occurrence in a mild condition has become one of the most popular methods of crosslinking among biopolymers [29–31]. Horseradish peroxidase (HRP) is one of the most commonly used peroxidases, known for its ability to gel in a matter of seconds [4, 28, 32].

Recently, antioxidants have gained considerable attention in biomedical applications because of their ability to act as reducing agents, hydrogen-donating antioxidants, free radical scavengers, and singlet oxygen quenchers [5, 33, 34]. Free radicals are involved in homeostasis and the transmission of messages. They are also produced naturally in the body, but unusually high levels cause chronic inflammation, which makes treatment difficult [33, 35]. Free radicals impair the metabolism of fibroblasts, keratinocytes, and endothelial cells by lipid peroxidation, which disrupts the wound healing process [5, 36, 37]. To eliminate the damaging effects of free radicals, various antioxidants have been used in wound healing [38, 39]. Taurine (2-aminoethanesulfonic acid, Tau) is a non-essential sulfur-containing amino acid found in almost all mammalian tissues, and it plays an important physiological and pathological role in various organ and tissue components [40–42]. This substrate is a powerful antioxidant that has positive effects on inflammation, cell proliferation, and collagen synthesis [36, 43, 44]. The valuable effects of Tau as an antioxidant in biological systems have been linked to its ability to stabilize biomembranes, scavenge ROS, and decrease peroxidation of unsaturated membrane lipids [44–46]. Tau has been used to prevent oxidative damage to skin wounds because it heals wounds [36].

Several studies have shown that gelatin affects cell migration and tissue organization during wound healing, and may cause epithelial tissue formation at the cellular level. However, in this study, we hypothesized that the development of Tau and hydroxyl phenol (Ph)-conjugated gelatin hydrogels would be a useful strategy to accelerate the healing of chronic wounds (Fig. 1a). The plan was to apply a gelatin-based dressing to promote endothelial cell (EC) proliferation, migration, and angiogenesis and achieve rapid wound healing (Fig. 1). The designed hydrogel was characterized using various methods. First of all, the biophysical properties were evaluated. Secondly, we investigated their effect on EC motil-

ity in two-dimensional (2D) and 3D systems with scratch and microparticle-based cell migration assays (Figs. 1b and 1c), respectively. Next, cell proliferation and morphology and expression of EC markers and proteins were determined to prove the functionality of conjugated Tau residues. Finally, wound closure and regenerated tissues were characterized (Fig. 1d).

Materials and methods

Materials

Gelatin (Type A, 300 bloom; ~50,000 and 100,000 Da), taurine, *N*-Hydroxysuccinimide (NHS), HRP (160 U/mg), sodium periodate, collagenase (170 U/mg), tyramine, water-soluble carbodiimide hydrochloride (WSCD), and 2-morpholinoethanesulfonic acid (MES) were purchased from Sigma (St. Luis. MO, USA). The H_2O_2 aqueous solution (30%, mass fraction) and other chemicals were obtained from Dr. Mojallali (Iran).

Cell culture

Endothelial cells (ECs) were cultured in Dulbecco's modified Eagle medium (DMEM) containing 10% (volume fraction) fetal bovine serum (FBS), 100 μg/mL penicillin, and 100 μg/mL streptomycin in a humidified atmosphere of 5% CO_2/95% air at 37 °C. Following the guidelines of the Ethics Committee on Research of Fasa University of Medical Sciences, cellular behaviors in the fabricated hydrogel were evaluated.

Preparation of taurine/phenol conjugated hydrogel

Gel-Ph-Tau was synthesized by amide-bond formation via carbodiimide-mediated condensation of the carboxyl groups of Gel with the amino groups of Tau using WSCD and NHS in MES buffer [43]. The Gel-Ph was synthesized in a similar way, by conjugation of the amino groups of gelatin with the carboxyl groups of tyramine. The amino group of Tau was conjugated with the carboxyl groups of gelatin. Briefly, gelatin was dissolved in 50 mmol/L MES buffer (pH 6.0) at 5 g/L. WSCD, NHS, tyramine, and Tau were added to this solution at 3.8, 3.2, 3.3, and 2.2 g/L, respectively. The amino reduction conjugation reaction was performed at room temperature for 16 h with mild stirring. To remove any remaining chemicals, the final solutions were dialyzed against deionized water using 12 kDa dialysis membranes, with the deionized water being changed every six hours. Afterward, modified Gel derivatives were lyophilized. The feasibility of conjugation of Ph and Tau contents to the backbone of the resultant polymers was determined through Fourier-transform infrared spectroscopy (FTIR). The degrees of substitution of Ph and Tau residues were determined spectrometrically (UV–VIS) at 275 nm, using the calibration curve of tyramine and at 570 nm by a ninhydrin reagent method, using a calibration curve pre-determined for known percentages of Tau substrate [41, 43, 47].

Fabrication of fluorescent microparticles

We used a double-orifice microfluidic device for microparticle fabrication [43, 48]. A combination of Gel-FluPh 5% (0.05 g/mL) and 40 U/mL HRP with a flow rate of 70 μL/min was inserted in 180-μm-diameter channels (inner channel). Liquid paraffin containing H_2O_2 and lecithin was introduced to the outer channel at a flow rate of 2 mL/min. The process of combining H_2O_2 and paraffin was carried out by homogenizing 60 mL of liquid paraffin and 0.6 mL of aqueous H_2O_2 solution (12 mol/L) for 10 min. After centrifuging at 3000 r/min to eliminate the surplus H_2O_2, the prepared emulsion was mixed with liquid paraffin containing 4% (mass fraction) lecithin at a ratio of 1:3. To separate microparticles from the liquid paraffin, the microparticles underwent several washing processes with the addition of calcium-free Krebs Ringer HEPES-buffered saline (CF-KRH buffer) at each step (including centrifugation at 1000 r/min for 1 min, followed by two washing steps at 1500 r/min for 4 min). Finally, the prepared Gel-FluPh microparticles were incubated for cell migration assay of hydrogels.

Hydrogel characteristics

Polydimethylsiloxane (PDMS)-based mold was used to fabricate cylindrical hydrogels for mechanical testing (5 mm diameter, 600 μL volume) [49]. We fabricated hydrogels of Gel-Ph and Gel-Ph-Tau at 3% (0.03 g/mL) in the presence of HRP and H_2O_2 at 2 U and 1 mmol/L, respectively; they were then kept at 25 °C for 1 h to complete polymerization and hydrogel network formation. Fabricated cylindrical hydrogels were placed in a compression machine (Zwick-Roell Z010, Germany). Additional cylindrical hydrogels were made identically to those created for the mechanical tests and were immersed in the PBS buffer for swelling and degradation tests [47]. To calculate the swelling ratio, we recorded the weight of each hydrogel before immersion (W_i) and removed the hydrogel immersed in PBS to record the wet weight (W_t), before which the surface water on the hydrogel was quickly removed using paper. Calculation of the swelling ratio was based on the following formula: $(W_t - W_i)/W_i$.

Hydrogels were soaked in PBS media containing 1 U/mL of collagenase type I for degradation study. The excess water from cylindrical hydrogels was wiped off, and the hydrogels were weighed until after 21 days.

Scratch migration assay

Endothelial cells (ECs) were seeded in a 24-well cell culture plate to form a cell monolayer with 80% confluency. Next, we used a yellow pipette tip to scratch cells on the tissue culture plates. To remove cell debris, wells were washed with culture media and then refilled with new culture medium. Culture media with four different conditions, including normal medium (Negative condition; group 1), Gel-Ph 3% (0.03 g/mL) (group 2), Gel-Ph 3% (0.03 g/mL) + soluble Tau 0.172% (0.00172 g/mL) (Sol Tau; group 3), and Gel-Ph-Tau 3% (0.03 g/mL) (group 4), were prepared and added to cultured cells. The amount of Tau in group 3 was equal to that in group 4 (Gel-Ph-Tau condition). Cell images were taken in the well plates immediately following the addition of new media and 24 h after that [50, 51].

Cell migration in hydrogels

Gel-FluPh microparticles were produced with the help of the microfluidic system to promote cell migration in 3D hydrogels, similar to the previously established method [43]. The stained ECs with green cell tracker dye were seeded onto microparticle surfaces by placing them in a non-adherent culture plate for 24 h. The cell-coated microparticles were embedded into 600 μL of prepared 3% (0.03 g/mL) gel-based hydrogels of different compositions, including Gel-Ph, Gel-Ph-Tau, and Gel-Ph+Sol Tau, which were polymerized by adding HRP (0.5 U/mL) and H_2O_2 (0.5 mmol/L). The culture medium was replaced every day following hydrogel placement in the non-adherent 24-well tissue culture dish. At different time intervals (0, 3, 7 days), cellular position was monitored using a fluorescence microscope (Labomed invert microscopic). The number of migrated cells and their average distance from the surface of microparticles were determined according to obtained images and Vernon and Sage's method [52].

Cellular behavior in hydrogels

Solutions of Gel-Ph, Gel-Ph-Tau, and Gel-Ph+Sol Tau (at concentrations of 0.03 g/mL) were mixed with ECs (2×10^6 cells/mL solution), HRP (0.5 U/mL), and H_2O_2 (0.5 mmol/L), and then 360 μL of each solution was poured into a 24-well cell culture plate. To probe cellular morphology, we fixed the encapsulated cells with 4% (0.04 g/mL) paraformaldehyde for 15 min and observed their morphology with a confocal laser scanning microscope (CLSM; Nikon C2, Nikon Corp, Tokyo, Japan). In addition, the hydrogels were exposed to the 0.5-mg/mL MTT (3-(4,5-dimethylthiazol-2-yl)-2,5-diphenyltetrazolium bromide) at specific time intervals (0, 3, 7 days) and incubated for 4 h. The MTT reagent was then replaced with dimethyl sulfoxide (DMSO) for color intensity measurements of DMSO at 450 nm by ELISA microplate readers.

Flow cytometry assay

On the 7th day of embedded EC incubation in hydrogels, ECs were recovered using collagenase. The recovered cells were washed three times with buffer (PBS and 5% bovine serum albumin. Cells were incubated on ice with mouse anti-human CD44 and CD31 antibodies (BD Biosciences, Franklin Lakes, NJ, USA) for 45 min in the dark. After washing cells three times with cold buffer, assays were performed using a BD Accuri C6 flow cytometer (BD Biosciences, CA, USA) [53].

Reverse transcription polymerase chain reaction (RT-PCR) assay

After seven days, the hydrogels containing ECs were immersed in collagenase type I to recover cells, followed by three washing steps with PBS. We accomplished RNA isolation using previously established methods [54, 55]. After adding TRIzol reagent (Invitrogen, Carlsbad, USA), we mixed lysed solutions with chloroform and centrifuged them (at 14,000*g*) for 30 min. Then, the supernatant was collected and mixed with an equal volume of isopropanol. The mRNA sediments were collected by centrifuging the resultant solution for 5 min at 14,000*g*. Next, a cDNA synthesis kit (AE301-02, TransGen Biotech) was applied to reverse transcribe the RNA into cDNA, which was then mixed with a supermix solution (AQ601-01, TransGen Biotech) and primers (Table 1). Finally, a 7500 real-time PCR system (Applied Biosystems, CA, USA) was used to perform the RT-PCR test.

Animal studies

The functionality of hydrogels for wound healing was assessed using a full-thickness excisional wound model [56, 57]. To this end, we divided 20 healthy adult male rats into four groups. Before we created wounds, the rats were anesthetized (0.1 mL ketamine 10% (volume fraction) and 0.05 mL xylazine). After shaving the rats' skin and washing it with ethanol 70%, we used a curved surgery scissor to create a full-thickness circular wound (diameter of 1 cm). The first group of rats, a negative control group, had not undergone any treatment. In the second group, the positive control group, animals were treated with paraffin gauze. In the third group, wound areas were covered with Gel-Ph. Finally, the fourth group of injured animals was treated with Gel-Ph-Tau. The wound areas were washed every 4 days with PBS and the dressing replaced with a fresh corresponding sample.

Table 1 Primers used in real-time PCR analysis

Gene	Primer (5–3)	Annealing temperature (°C)
VEGF	CCT CCG AAA CCA TGA ACT TT	57
	TTC TTT GGT CTG CAT TCA CAT T	
bFGF	TCT GGC AGT TCC TTA TGA TAG	58
	AAA TAC AAC TCC CAT CAC CAG	
Ang 1	TTC CTT TCC TTT GCT TTC CTC	59
	CTGCAGAGCGTTTGTGTTGT	
GAPDH	CCT GTA CGC CAA CAC AGT GC	57
	ATA CTC CTG CTT GCT GAT CC	

At time intervals of 0, 4, 8, and 12 days, wound reduction was tracked with a digital camera. Quantitative analysis was performed with a combination of image analysis and the following equation [36]:

$$\text{Wound closure} = \left(1 - \frac{\text{Wound area at the given time}}{\text{Initial wound area}}\right) \times 100\%.$$

Histopathology

At the end of the study, the animals were euthanized by anesthetic overdose (100 mg ketamine and 25 mg xylazine/kg body weight). The wound site was excised, and the treated tissue was used for histological assessment. Just after wound isolation, the specimens were fixed with paraformaldehyde 4%, gradually dehydrated (using ethanol 50% to 95%), and embedded in paraffin. To assess the privileged histologically healing condition, the specimens were sectioned in 6-μm slices by a rotary microtome and stained with hematoxylin–eosin (H&E) and Masson's trichrome (MT) stain. The stained samples were observed by an independent pathologist using a light microscope.

Statistical analysis

We used the two-tail *T* test to analyze quantitative data using an ANOVA to determine statistical significance ($P<0.05$). Resultant data were presented as means with standard deviations (SDs).

Results and discussion

Characterization of synthesized Gel-Ph-Tau

The Ph contents of the resultant Gel-Ph-Tau and Gel-Ph were determined to be 1.81×10^{-4} mol-Ph/g-Gel-Ph-Tau and 1.94×10^{-4} mol-Ph/g-Gel-Ph, using an ultraviolet–visible spectrometer. The Tau conjugated was 4.6×10^{-5} mol-Tau/g-Gel-Ph-Tau (or 5.75 mg Tau/g-Gel-Ph-Tau). The FTIR spectra (Fig. 2a) indicated the characteristic peaks of Gel, including a strong band at 1620–1640 cm^{-1} proving the C=C groups of Ph, a hydroxyl O–H broadband in the range of 3000–3400 cm^{-1}, and an ether aliphatic C–H stretching band (2840–2910 cm^{-1}). The peak at 1190 cm^{-1} contributed to stretching vibrations of carboxylic functional groups related to aliphatic ether. Also, the spectra of designed hydrogels showed that the Gel-based fingerprint bands at 1250–1280 cm^{-1} were related to the C–N and N–H bands at 1633 cm^{-1} (typical of amide I), 3420 cm^{-1} (amide A), and 29 150 cm^{-1} (amide B). The peaks for N–H stretching vibration of amine I, carbonyl stretch of amide II, and amide III appeared at 1637, 1558, and 1414 cm^{-1}, respectively. The peaks for asymmetric and symmetric stretching vibration bands of the sulfonate (O=S=O) group were at 1125 and 1181 cm^{-1}. These results indicated that Tau was conjugated onto the Gel-Ph-Tau chain without breaking the structure.

Physical characteristics of hydrogels

We used prepared cylindrical hydrogels for characterization of the physical properties of the samples (Fig. 2b). As shown in Fig. 2c, the Gel-Ph and Gel-Ph-Tau were tested under compressive stress–strain profiles up to 80% strain. Unlike Gel-Ph, which was resistant to 128 kPa, the Gel-Ph-Tau hydrogel was shown to be resistant to 212 kPa. The swelling properties of the prepared Gel-based hydrogels are shown in Fig. 2d. A dramatic and equal level of swelling were observed from 0 to 8 h in both Gel-Ph and Gel-Ph-Tau hydrogels. The swelling kinetics of both hydrogels reached saturation with an equilibrium swelling ratio of 3.02 and 2.67, respectively, after 12 h; this remained static through the extended incubation time until 36 h, the point at which the equilibrium state of hydrogels was determined. In addition, the biodegradability of Gel-Ph and Gel-Ph-Tau was evaluated by soaking the formed cylindrical hydrogels in the PBS buffer containing

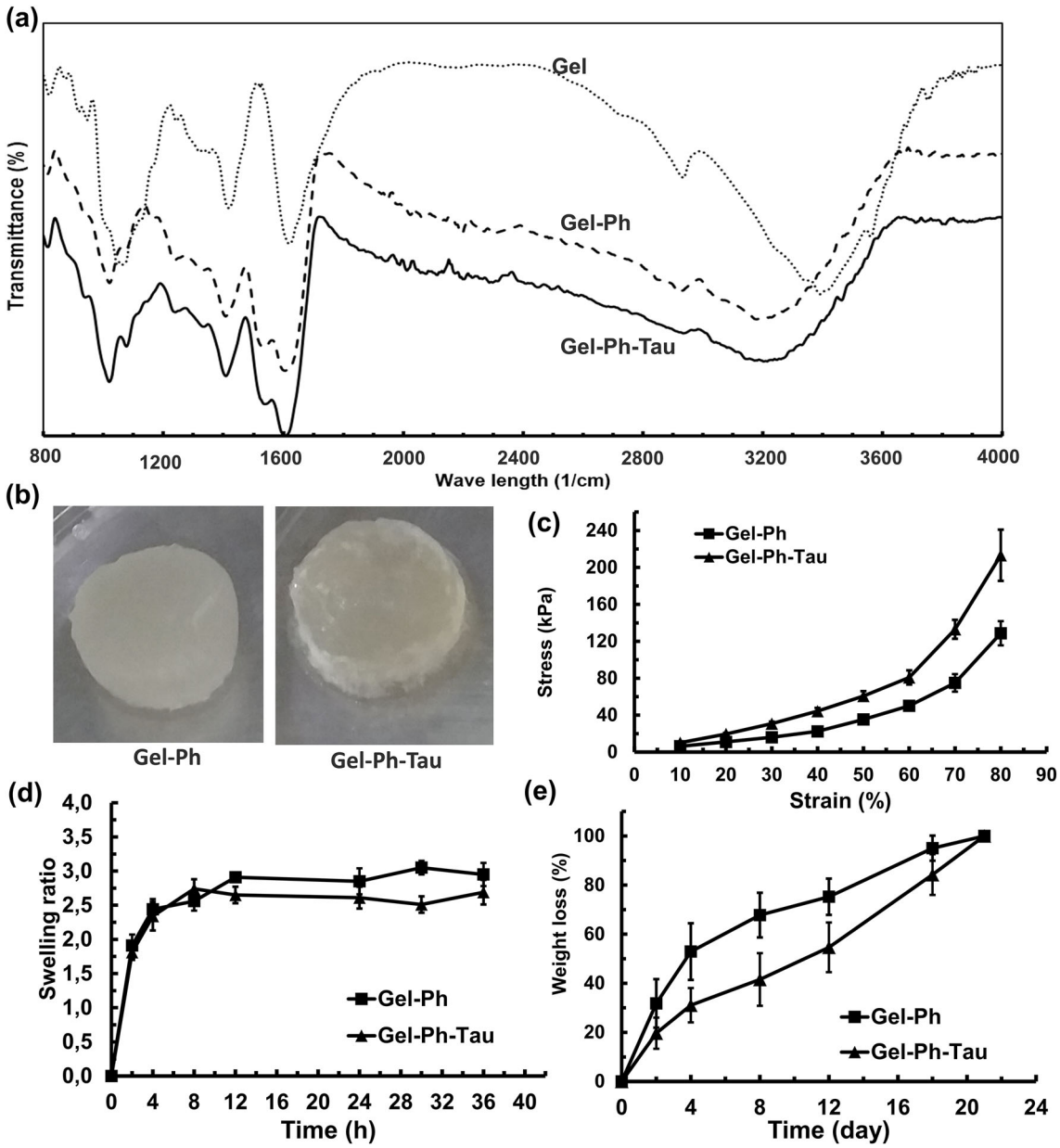

Fig. 2 **a** Fourier-transform infrared spectroscopy (FTIR) analysis of synthesized substrates for hydrogels production, **b** photographs of prepared Gel-based hydrogels, **c** compression assay, **d** swelling kinetics, and **e** degradation assay of Gel-Ph and Gel-Ph-Tau. The data are representative of the averages obtained by triple replicating each hydrogel

collagenase. Figure 2e shows that the hydrogels completely degraded within 21 days. Interestingly, the weight loss speed of Gel-Ph was faster than that of Gel-Ph-Tau at various time points, but both degraded completely on day 21. Therefore, the conjugation of Tau and covalent crosslinking among Ph moieties did not inhibit bioactivity of collagenase, and the Gel molecules were broken and dissociated by collagenase treatment. In summary, Gel-Ph-Tau has superior mechanical properties, a lower swelling ratio, and a slower degradation rate, possibly due to greater stability provided by the presence of Tau molecules in the polymer chains.

Scratch migration assay

We characterized ECs through time profiling experiments to determine the effects of hydrogels on their motility and morphology. In the presence of immobilized or soluble Tau in hydrogels, ECs covered the scratched (cell-free) areas of culture dishes after 24 h, whereas the control and Gel-Ph groups covered only 42% and 65% of the scratched areas, respectively (Fig. 3). However, the soluble form of Tau caused fewer migrated cells, suggesting that using conjugated Ph moieties as a backbone for Tau affected cell motility. In either case, it

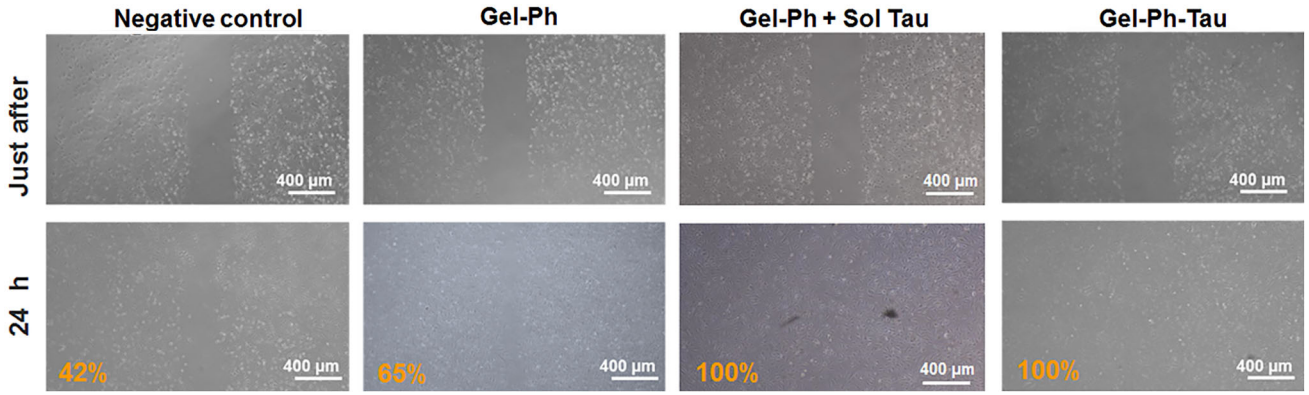

Fig. 3 Microscopic images of endothelial cells (ECs) during the scratch migration assay. Cells were cultured in normal DMEM medium without adding Gel-Ph or Tau in the media as a negative control; or cultured in media containing 3% (0.03 g/mL) of Gel-Ph, Gel-Ph+soluble taurine (Sol Tau), and Gel-Ph-Tau, respectively. The data are representative of the averages obtained by triple replicating each hydrogel

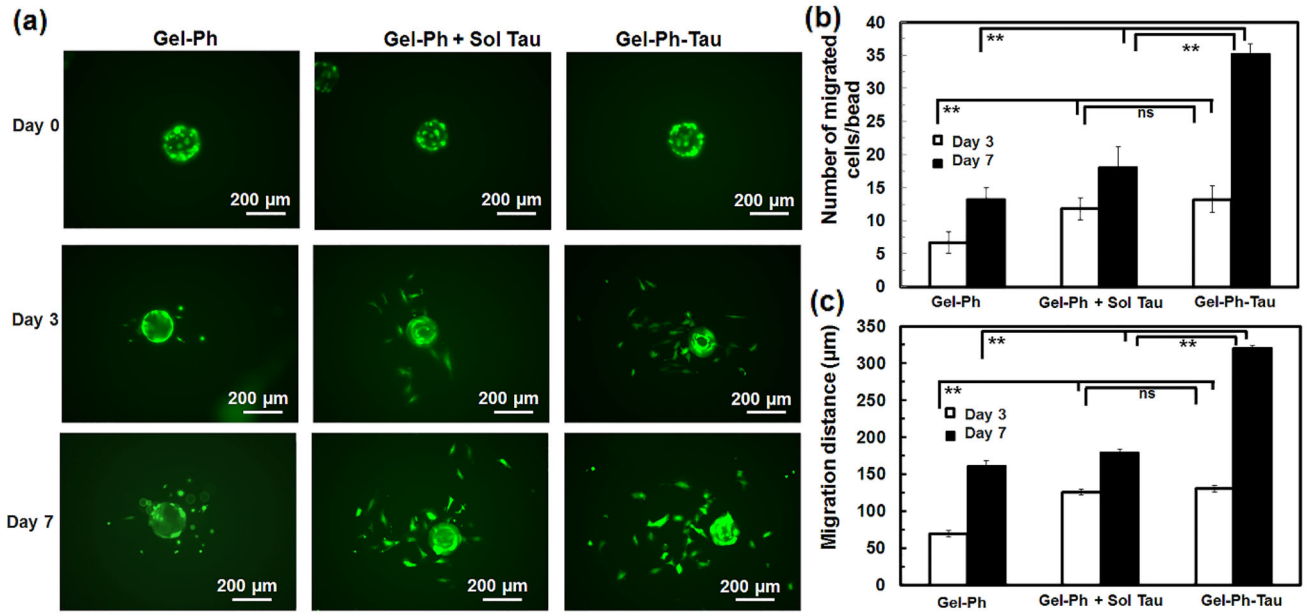

Fig. 4 Endothelial cell (EC) migration in 3D hydrogels: **a** micrographs of cell migration in 3D hydrogels on days 0, 3, and 7; **b** numbers of migrated cells; **c** migration distance from the microparticle surface in different hydrogels. The data are representative of the averages obtained for 20 replicated microparticles in each hydrogel condition. Distances were measured utilizing a radial grid of 18 radii centered over the photomicrograph of each microparticle

can be concluded that taurine's existence in hydrogels promoted cell migration, which agrees with previous studies [46]. The images displayed in Fig. 3 do not show that the ECs exhibited any significant differences in their morphologies under different conditions.

Microparticle-based cell migration assay

We investigated the migration of ECs in the 3D culture microenvironment by seeding ECs on microparticle surfaces and embedding them in the evaluation hydrogel matrixes (Fig. 1c). The effects of the different hydrogel types, including Gel-Ph, Gel-Ph+Sol Tau, and Gel-Ph-Tau on cell migration were examined at intervals of 0, 3, and 7 days, at the same concentration of 3% (0.03 g/mL) for Gel derivatives. One can see in Fig. 4a that at the 3rd and 7th days of migration, the Gel-Ph-Tau influenced both distance and number of migrated cells, which are indicators of the response to migration (Figs. 4b and 4c). Among the different hydrogels (Gel-Ph, Gel-Ph-Tau, and Gel-Ph+Sol Tau), the furthest migration distance of cells was 330 μm (in Gel-Ph-Tau), with an average number of 35 migrated cells per microparticle. Compared with a Gel-Ph hydrogel crosslinked with Tau, the average migration distance

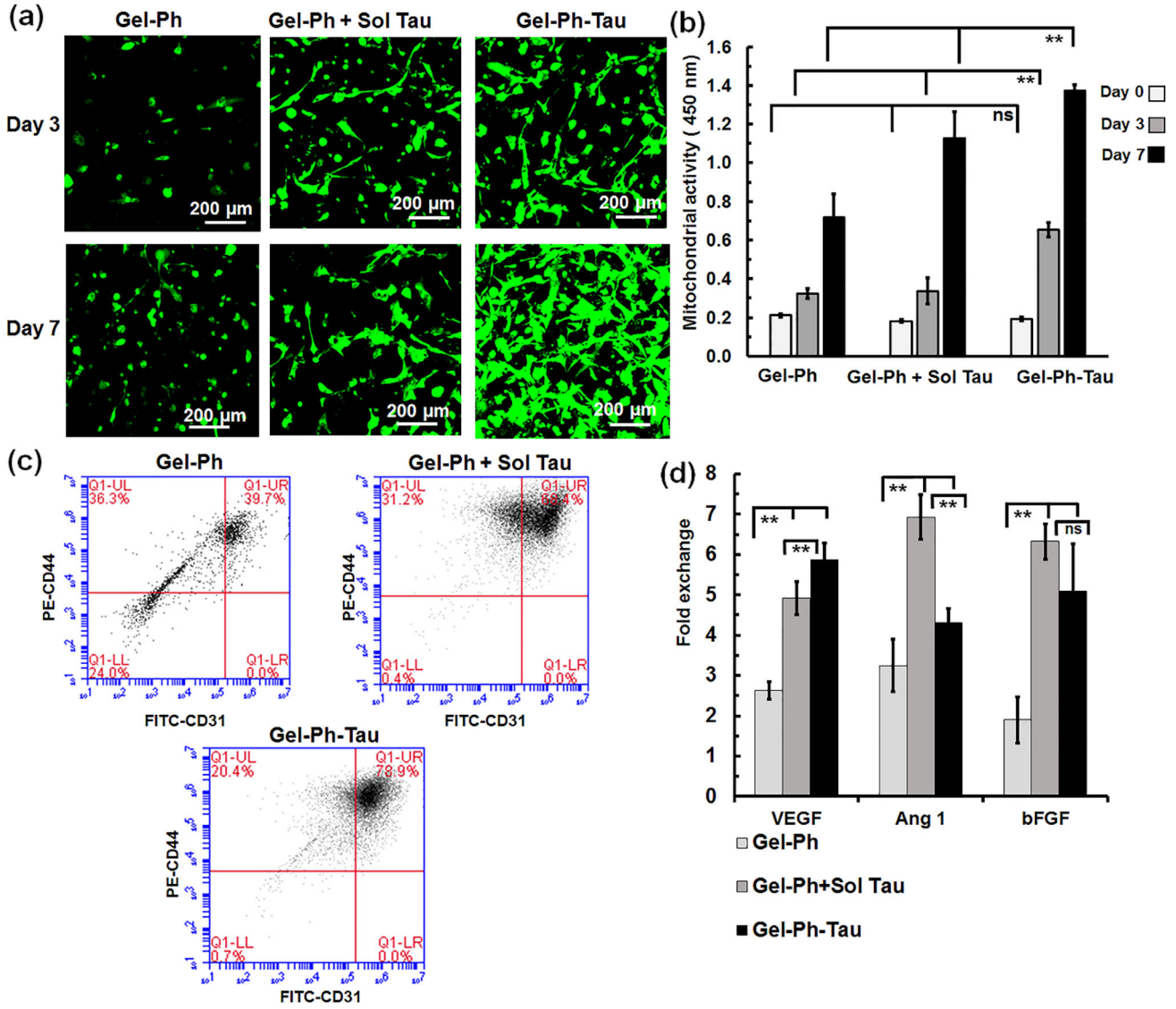

Fig. 5 **a** Morphological changes of embedded endothelial cells (ECs) in Gel-Ph, Gel-Ph+Sol Tau, and Gel-Ph-Tau on days 3 and 7. **b** Cell proliferation based on mitochondrial activity for these groups on days 0, 3, and 7. **c** CD44 and CD31 expression of embedded ECs characterized by flow cytometry on day 7. The top, left, and right top portions show positive CD44, CD31, and double-positive CD44 and CD31, respectively. **d** Expression of VEGF, Ang 1, and bFGF by embedded ECs characterized by RT-PCR. The data are representative of the averages obtained by triple replicating each hydrogel

and number of cells in the Gel-Ph hydrogel were 50% and 63% lower, respectively, on day 7 of encapsulation (Figs. 4a–4c). On day 3, the ECs migrated almost equally in hydrogels containing crosslinked or soluble Tau; however, the crosslinked Tau induced cells to migrate farther by day 7 (Fig. 4c). The longer migration distances on day 7 indicated the long-term effectiveness of conjugated Tau in the Gel-Ph-Tau hydrogel. In brief, the carbodiimide conjugation of Tau in the Gel-Ph-Tau substrate played a larger role in the migration and survival of ECs, as evidenced by the high average number of migrating cells in hydrogels functionalized with Tau residues. It should be noted that the effect of covalently conjugated Tau in Gel-Ph is comparable to that in the previous studies conducted on other kinds of cells and hydrogels containing Tau residues [5, 27].

Analysis of cells encapsulated in hydrogels

CLSM was used to observe the morphology of the cells within the Gel-Ph, Gel-Ph+Sol Tau, and Gel-Ph-Tau. The embedded cells in Gel-Ph+Sol Tau and Gel-Ph-Tau hydrogels started developing a spindle-shaped structure and cytoplasmic extensions by day 3, as shown in Fig. 5a. The cells

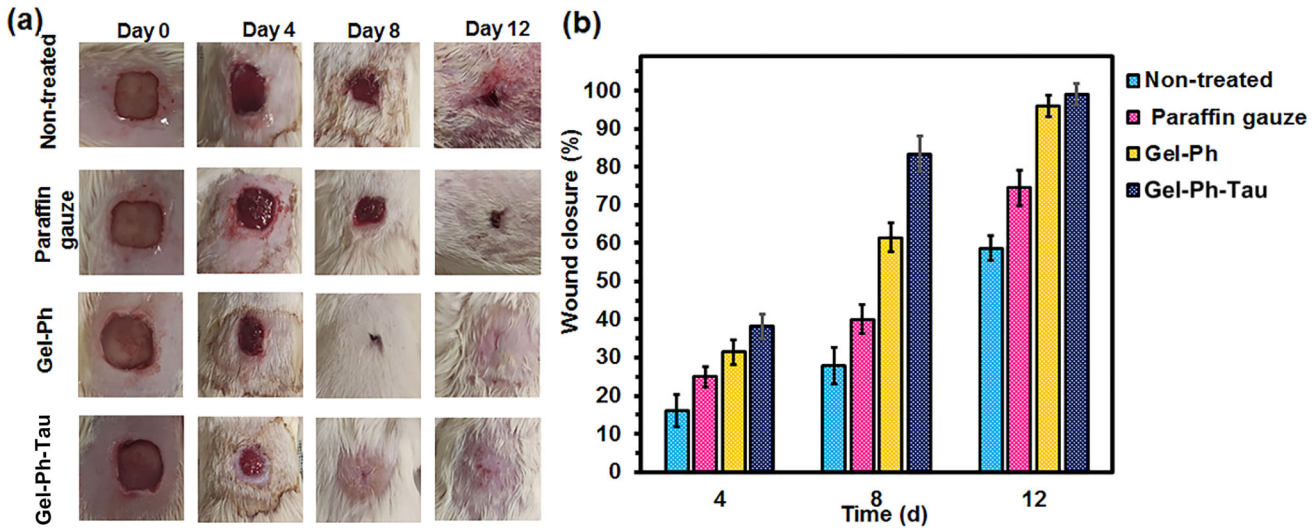

Fig. 6 In vivo models of wound healing. **a** The appearance of wounds treated with paraffin gauze, Gel-Ph, and Gel-Ph-Tau after 4, 8, and 12 days. Non-treated wounds are considered a negative control. **b** Percentage of wound closure for these groups in monitored time lapse

in the Gel-Ph hydrogel maintained a sphere-like shape, in contrast to those with Tau residues. Based on the shape of embedded cells, the presence of Tau in hydrogels enables embedded ECs to form capillary-like structures. It has been reported in other studies that cytoplasmic extension is essential to enhancing angiogenesis [8, 13]. We observed this in both Gel-Ph+Sol Tau and Gel-Ph-Tau hydrogels on day 7; it was an indication that the presence of Tau residues provided favorable conditions for angiogenesis and recapitulation of ECM properties. In contrast to soluble Tau, the covalently immobilized Tau residues showed a significantly higher number of cells with the cytoplasmic extension on day 7 of encapsulation. Furthermore, Fig. 5b shows that Gel-Ph-Tau hydrogel resulted in higher cell proliferation on days 3 and 7 than Gel-Ph and Gel-Ph+Sol Tau. As determined by the assay, the covalently crosslinked Tau in Gel-Ph-Tau is a suitable method of obtaining a more biomimetic hydrogel with angiomodulatory properties.

Expression of EC surface proteins

We conducted this study to better understand the observed behavior of embedded cells under the influence of Tau and examine how this residue could interact with the surrounding microenvironment in terms of regulating ECs through cell receptor interactions. For this purpose, we quantified the CD44 and CD31 expression of embedded cells in Gel-Ph, Gel-Ph+Sol Tau, and Gel-Ph-Tau on day 7 (Fig. 5c). Unlike ECs embedded in Gel-Ph, which showed an insignificant degree of CD44 and CD31 expression (39.7%), these markers were highly positive for cells in Gel-Ph+Sol Tau and Gel-Ph-Tau hydrogels (68.4% and 78.9%, respectively). The presence of high levels of CD44 and CD31 in the Gel-Ph+Sol Tau and especially Gel-Ph-Tau hydrogels can be attributed to EC proliferation and morphogenesis in the designed hydrogels [43, 58].

Degree of angiogenesis factors

The RT-PCR assay was implemented to study the angiogenesis factors of bFGF, Ang1, and VEGF [59, 60]. The results were normalized to ECs cultured in polystyrene culture dishes. Figure 5d shows that in hydrogels that included Tau, the expression of VEGF, Ang1, and bFGF was significantly higher than in the control group (polystyrene culture dish) or Gel-Ph condition. This phenomenon was correlated with results obtained from morphological investigation of ECs encapsulated in hydrogels. The availability of a higher amount of positive charged growth factors (including bFGF and VEGF) within the prepared Gel-Ph-Tau gel matrix indicated that immobilization of Tau could localize growth factors released by encapsulated cells within the hydrogel microenvironment. Based on these results and those described in previous sections, we can conclude that the presence of Tau residues can increase angiogenesis factors and lead to higher EC proliferation, migration, and morphogenesis (Figs. 4 and 5).

Wound dressings

Figure 6a illustrates the wound-healing process in the following groups at different time points: non-treated (negative control), paraffin gauze (positive control), Gel-Ph, and Gel-Ph-Tau. In the control group, wounds were still fresh and bleeding on day 4. On the same day, the wound margins of

the groups treated with Gel-Ph and Gel-Ph-Tau were unclear, showing marginal regeneration [36]. There was no sign of inflammation or infection in any of the groups. Additionally, we determined wound closure for each group by comparing the percentage of wound reduction at intervals of 0, 4, 8, and 12 days. Figure 6b shows that the highest and lowest percentages of wound closure were obtained in the Gel-Ph-Tau and non-treated groups, respectively, at all time points. Compared to the negative control, which exhibited 59% wound closure on day 12, 75% wound closure was achieved in the positive control (paraffin gauze). The Gel-Ph and Gel-Ph-Tau wound dressings resulted in 95% and 100% wound closure, indicating the efficacy of Tau and the importance of the scaffold composite.

Histological analysis

We carried out histopathological analyses of the skin wounds for significant skin features such as tissue regeneration, collagen deposition in the tissue sections, and angiogenesis, using H&E and MT staining. The H&E staining in the normal group showed a distinguishable, typically thicker, stratified epidermis, and dermis layer, with characteristics such as well-organized epidermal papillae and ridges with visible stratum corneum and basale. Moreover, the components of the dermis layer, such as hair follicles, sebaceous and sweat glands, arrector pili muscles, adipose tissue, and capillaries were well-formed. In the gauze-treated wound group, we observed an incomplete epidermis with less visible regular stratum layers and incompletely defined epidermal papillae, which are incompatible with epidermal ridges (Fig. 7). Furthermore, in the gauze-treated wound group, the presence of an external agent caused an influx of inflammatory cells in the wound area. The absence of skin in this area prevented the hair follicles from being juxtaposed and also, there was distention of a few follicles without any glands. Histopathology of wounds in the Gel-Ph-hydrogel-treated group revealed restoration of the epidermis and enhancement of the thin epidermal layer post treatment. After treatment with Gel-Ph-Tau, we were able to see better recovery of skin layers, a loose crust of dermal layers, the presence of sweat and sebaceous glands, and rearrangement of hair follicles (Fig. 7). Angiogenesis is imperative for complete wound repair. The histopathological results indicated that the capillary formation index in the Gel-Ph-Tau group was higher than in other groups (Fig. 8). The light microscope MT-stained sections showed that the loosely packed collagen fibers, which were detected at the edge of treated groups, had irregular alignment. The collagen fibers in the dermal layer were sparser at the edge of wounds treated with Gel-Ph-Tau. However, the fibers tended to be denser when approaching the center (Fig. 8). Unlike gauze-treated wounds, the collagen fibers at

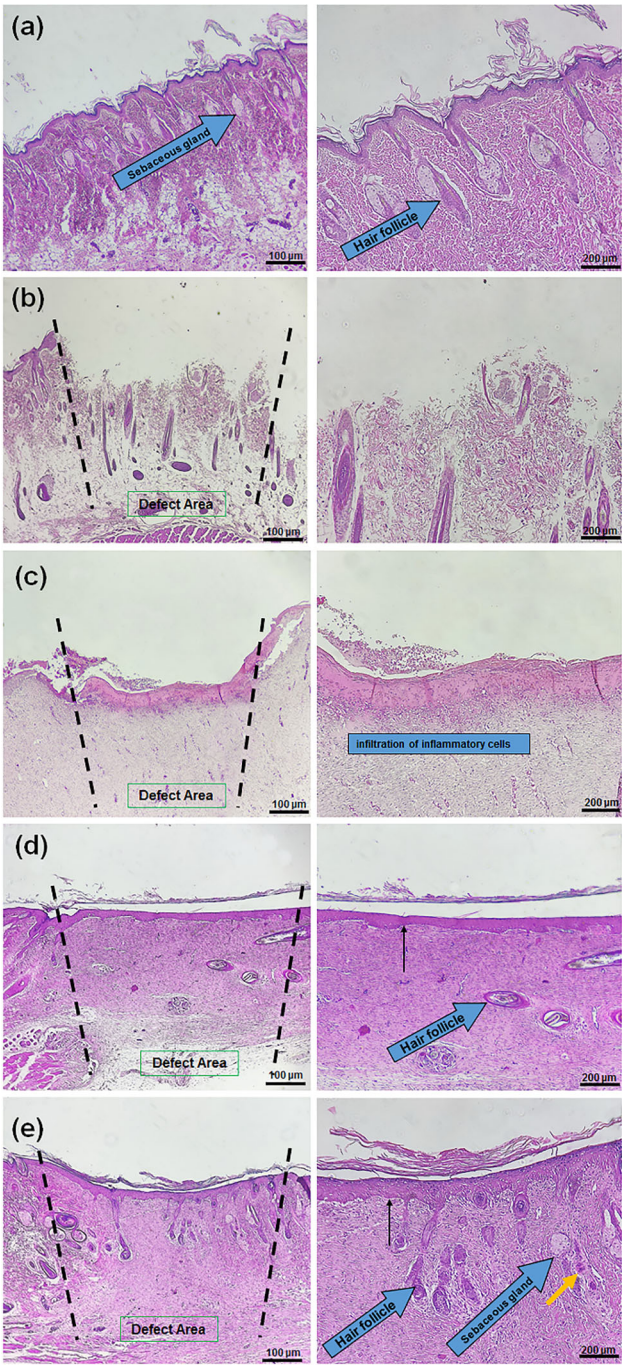

Fig. 7 Wound-healing hematoxylin–eosin (H&E)-stained microscopic sections in rats on day 12. **a** Control. Normal back-skin tissue characteristics such as epidermis and dermis, sebaceous glands, and hair follicles can be recognized clearly (blue arrows). **b** Wound after skin injury; the epidermis and dermis layers are damaged, and the skin has lost its integrity. **c** Sterile-gauze-treated wound. Sterile gas as an external agent causes a heavy flow of immune-system inflammatory cells into the wound area. **d** Gel-Ph-hydrogel-treated wound. The visible epidermis and dermis; a few hair follicles of the sebaceous glands are distinguishable. **e** Gel-Ph-Tau-treated wound. Dermal papillae with their ridge (black arrow) and neovascularization (yellow arrow) are visible. Each row represents a hydrogel group at two magnifications

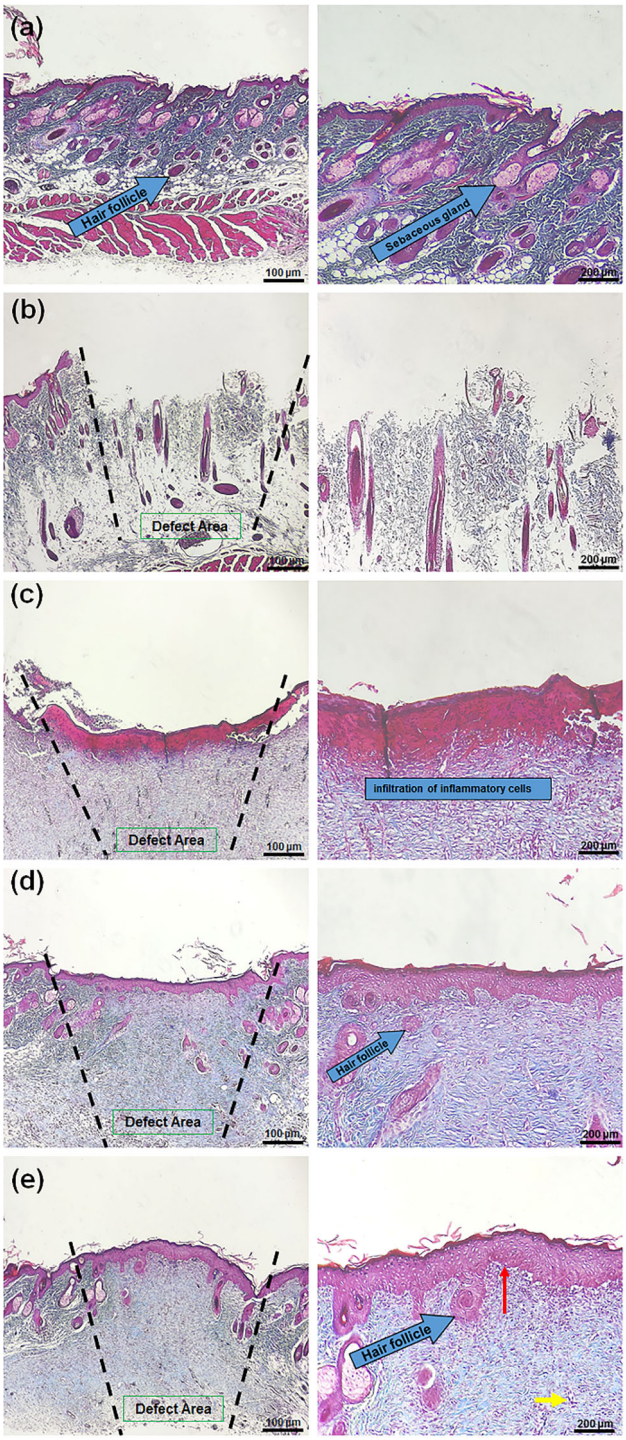

Fig. 8 Histopathological analysis of the Masson's trichrome (MT) stained skin at the end of the 12th post-wounding day. **a** Control. Regular dense collagen fibers stained blue-green and nuclei and cytoplasm stained red. **b** Wound. Collagen fiber deposition and irregular form of skin layers after injury. **c** Sterile-gauze-treated wound. Presence of inflammatory cells with loosely packed collagen was observed. **d** Gel-Ph-hydrogel-treated wound. Dense collagen fibers with parallel alignment are distinguishable. **e** Gel-Ph-Tau-treated wound, showing no scar, fewer inflammatory cells, more hair follicles, fibroblasts, and blood vessels, and extensive collagen fibers in a regular arrangement. Each row represents a hydrogel group at two magnifications

the center of Gel-Ph-Tau-treated wounds were reconstructed and densely packed, with a parallel arrangement.

Future work

Matrix metalloproteinases (MMPs) play an important role in skin regeneration and modification by influencing cell behavior, apoptosis, and proliferation [61]. MMPs have been shown to activate cellular factors such as growth factors, cytokines, and chemokines. Moreover, their involvement in all wound-healing phases has been proven, increasing their importance of research [62, 63]. Due to their importance, we suggest that the effect of the proposed hydrogel on MMPs should be investigated.

Conclusions

Based on this study, we found that a functionalized Gel hydrogel with Tau is beneficial to wound healing, as it promotes the proliferation, migration, and morphogenesis of ECs and skin wound tissue regeneration. The conjugation of Tau in a Gel backbone for a prepared HRP-mediated hydrogel improved the gel's physical properties by moderating degradation and improving mechanical properties. The Gel-Ph-Tau hydrogel promotes a significant increase in the number of migrated ECs, as well as average migration distance. In addition to high cell motility, a robust cytoskeleton extension, high expression of CD44 and CD31 cell receptors and angiogenic proteins, and results of in vivo analyses support the positive effects of Gel-Ph-Tau hydrogel bioactivity as an angiogenesis aid in tissue regeneration applications. In summary, the results indicate promising prospects for functionalized Gel-based hydrogels with taurine for skin tissue repair.

Author contributions FR, AG (Aida Goodarzi), and MK contributed to conceptualization; FN, NA, FR, SS, and SH contributed to formal analysis and investigation; NA, FN, and AG (Arash Goodarzi) contributed to writing—original draft preparation; AG (Arash Goodarzi) and MK contributed to supervision.

Declarations

Conflict of interest The authors declare that they have no conflict of interest.

Ethical approval All institutional and national guidelines for the care and use of laboratory animals were followed. Animal use and care were approved with National Ethics Committee of Fasa University of Medical Sciences (Ethical code: IR.FUMS.REC.1399.160) and were performed in accordance with the university's guidelines. Furthermore, all animal experiments comply with the National Institutes of Health guide for the care and use of laboratory animals (NIH Publications No. 8023, revised 1978).

Data availability The datasets used and/or analyzed during the current study are available from the corresponding authors on reasonable request.

References

1. Dong RN, Guo BL (2021) Smart wound dressings for wound healing. Nano Today 41:101290. https://doi.org/10.1016/j.nantod.2021.101290
2. Masson-Meyers DS, TaM A, Caetano GF et al (2020) Experimental models and methods for cutaneous wound healing assessment. Int J Exp Pathol 101(1–2):21–37. https://doi.org/10.1111/iep.12346
3. Farahani M, Shafiee A (2021) Wound healing: from passive to smart dressings. Adv Healthc Mater 10(16):e2100477. https://doi.org/10.1002/adhm.202100477
4. Liang YP, He JH, Guo BL (2021) Functional hydrogels as wound dressing to enhance wound healing. ACS Nano 15(8):12687–12722. https://doi.org/10.1021/acsnano.1c04206
5. Zhang SH, Hou JY, Yuan QJ et al (2020) Arginine derivatives assist dopamine-hyaluronic acid hybrid hydrogels to have enhanced antioxidant activity for wound healing. Chem Eng J 392:123775. https://doi.org/10.1016/j.cej.2019.123775
6. Rodrigues M, Kosaric N, Bonham CA et al (2019) Wound healing: a cellular perspective. Physiol Rev 99(1):665–706. https://doi.org/10.1152/physrev.00067.2017
7. Han G, Ceilley R (2017) Chronic wound healing: a review of current management and treatments. Adv Ther 34(3):599–610. https://doi.org/10.1007/s12325-017-0478-y
8. Khanmohammadi M, Sakai S, Taya M (2019) Characterization of encapsulated cells within hyaluronic acid and alginate microcapsules produced via horseradish peroxidase-catalyzed crosslinking. J Biomat Sci-Polym E 30(4):295–307. https://doi.org/10.1080/09205063.2018.1562637
9. Wang P, Huang BS, Horng HC et al (2018) Wound healing. J Chin Med Assoc 2(81):94–101
10. Rieger KA, Birch NP, Schiffman JD (2013) Designing electrospun nanofiber mats to promote wound healing - a review. J Mater Chem B 1(36):4531–4541. https://doi.org/10.1039/c3tb20795a
11. Alven S, Aderibigbe B (2019) Combination therapy strategies for the treatment of malaria. Molecules 24(19):3601. https://doi.org/10.3390/molecules24193601
12. Opt Veld RC, van den Boomen OI, Lundvig DMS et al (2018) Thermosensitive biomimetic polyisocyanopeptide hydrogels may facilitate wound repair. Biomaterials 181(392):401. https://doi.org/10.1016/j.biomaterials.2018.07.038
13. Lin KS, Wang SY, Fan LJ et al (2017) Adipose-derived stem cells seeded in pluronic F-127 hydrogel promotes diabetic wound healing. J Surg Res 217:63–74. https://doi.org/10.1016/j.jss.2017.04.032
14. Zhu JM, Marchant RE (2011) Design properties of hydrogel tissue-engineering scaffolds. Expert Rev Med Devic 8(5):607–626. https://doi.org/10.1586/Erd.11.27
15. Catanzano O, Quaglia F, Boateng JS (2021) Wound dressings as growth factor delivery platforms for chronic wound healing. Expert Opin Drug Del 18(6):737–759. https://doi.org/10.1080/17425247.2021.1867096
16. Jo H, Yoon M, Gajendiran M et al (2020) Recent strategies in fabrication of gradient hydrogels for tissue engineering applications. Macromol Biosci 20(3):1900300. https://doi.org/10.1002/mabi.201900300
17. Hsu YY, Liu KL, Yeh HH et al (2019) Sustained release of recombinant thrombomodulin from cross-linked gelatin/hyaluronic acid hydrogels potentiate wound healing in diabetic mice. Eur J Pharm Biopharm 135:61–71. https://doi.org/10.1016/j.ejpb.2018.12.007
18. Dang LH, Huynh NT, Pham NO et al (2019) Injectable nanocurcumin-dispersed gelatin-pluronic nanocomposite hydrogel platform for burn wound treatment. B Mater Sci 42(2):71. https://doi.org/10.1007/s12034-019-1745-0
19. Khamrai M, Banerjee SL, Paul S et al (2019) Curcumin entrapped gelatin/ionically modified bacterial cellulose based self-healable hydrogel film: an eco-friendly sustainable synthesis method of wound healing patch. Int J Biol Macromol 122:940–953. https://doi.org/10.1016/j.ijbiomac.2018.10.196
20. Mansoori-Kermani A, Khalighi S, Akbarzadeh I et al (2022) Engineered hyaluronic acid-decorated niosomal nanoparticles for controlled and targeted delivery of epirubicin to treat breast cancer. Mater Today Bio 16:100349. https://doi.org/10.1016/j.mtbio.2022.100349
21. Singaravelu S, Ramanathan G, Raja MD et al (2016) Biomimetic interconnected porous keratin–fibrin–gelatin 3D sponge for tissue engineering application. Int J Biol Macromol 86:810–819. https://doi.org/10.1016/j.ijbiomac.2016.02.021
22. Benskin LL (2018) Evidence for polymeric membrane dressings as a unique dressing subcategory, using pressure ulcers as an example. Adv Wound Care 7(12):419–426. https://doi.org/10.1089/wound.2018.0822
23. Ye HL, Cheng JW, Yu K (2019) In situ reduction of silver nanoparticles by gelatin to obtain porous silver nanoparticle/chitosan composites with enhanced antimicrobial and wound-healing activity. Int J Biol Macromol 121:633–642. https://doi.org/10.1016/j.ijbiomac.2018.10.056
24. Ndlovu SP, Ngece K, Alven S et al (2021) Gelatin-based hybrid scaffolds: promising wound dressings. Polymers 13(17):2959. https://doi.org/10.3390/polym13172959
25. Dias JR, Baptista-Silva S, De Oliveira CMT et al (2017) In situ crosslinked electrospun gelatin nanofibers for skin regeneration. Eur Polym J 95:161–173. https://doi.org/10.1016/j.eurpolymj.2017.08.015
26. Rath G, Hussain T, Chauhan G et al (2016) Development and characterization of cefazolin loaded zinc oxide nanoparticles composite gelatin nanofiber mats for postoperative surgical wounds. Mat Sci Eng C Mater 58:242–253. https://doi.org/10.1016/j.msec.2015.08.050
27. Campiglio CE, Contessi Negrini N, Fare S et al (2019) Cross-linking strategies for electrospun gelatin scaffolds. Materials 12(15):2476. https://doi.org/10.3390/ma12152476
28. Badali E, Hosseini M, Mohajer M et al (2021) Enzymatic crosslinked hydrogels for biomedical application. Polym Sci Ser A 63(Suppl 1):S1–S22. https://doi.org/10.1134/S0965545x22030026
29. Khanmohammadi M, Dastjerdi MB, Ai A et al (2018) Horseradish peroxidase-catalyzed hydrogelation for biomedical applications. Biomater Sci 6(6):1286–1298. https://doi.org/10.1039/c8bm00056e
30. Davachi SM, Haramshahi SMA, Akhavirad SA et al (2022) Development of chitosan/hyaluronic acid hydrogel scaffolds via enzymatic reaction for cartilage tissue engineering. Mater Today Commun 30:103230. https://doi.org/10.1016/j.mtcomm.2022.103230
31. Badali E, Hosseini M, Varaa N et al (2022) Production of uniform size cell-enclosing silk derivative vehicles through coaxial microfluidic device and horseradish crosslinking reaction. Eur Polym J 172:111237. https://doi.org/10.1016/j.eurpolymj.2022.111237
32. Liu Y, Wong CW, Chang SW et al (2021) An injectable, self-healing phenol-functionalized chitosan hydrogel with fast gelling property and visible light-crosslinking capability for 3D printing. Acta Biomater 122:211–219. https://doi.org/10.1016/j.actbio.2020.12.051
33. Deng LL, Du CZ, Song PY et al (2021) The role of oxidative stress and antioxidants in diabetic wound healing. Oxid Med Cell Longev 2021:8852759. https://doi.org/10.1155/2021/8852759

34. Xu ZJ, Han SY, Gu ZP et al (2020) Advances and impact of antioxidant hydrogel in chronic wound healing. Adv Healthc Mater 9(5):1901502. https://doi.org/10.1002/adhm.201901502
35. Zdunska K, Dana A, Kolodziejczak A et al (2018) Antioxidant properties of ferulic acid and its possible application. Skin Pharmacol Phys 31(6):332–336. https://doi.org/10.1159/000491755
36. Farzamfar S, Naseri-Nosar M, Samadian H et al (2018) Taurine-loaded poly (ε-caprolactone)/gelatin electrospun mat as a potential wound dressing material: in vitro and in vivo evaluation. J Bioact Compat Pol 33(3):282–294. https://doi.org/10.1177/0883911517737103
37. Vittorazzi C, Endringer DC, De Andrade TU et al (2016) Antioxidant, antimicrobial and wound healing properties of *Struthanthus vulgaris*. Pharm Biol 54(2):331–337. https://doi.org/10.3109/13880209.2015.1040515
38. Li M, Chen J, Shi MT et al (2019) Electroactive anti-oxidant polyurethane elastomers with shape memory property as non-adherent wound dressing to enhance wound healing. Chem Eng J 375:121999. https://doi.org/10.1016/j.cej.2019.121999
39. Qu J, Zhao X, Liang YP et al (2018) Antibacterial adhesive injectable hydrogels with rapid self-healing, extensibility and compressibility as wound dressing for joints skin wound healing. Biomaterials 183:185–199. https://doi.org/10.1016/j.biomaterials.2018.08.044
40. Lambert IH, Kristensen DM, Holm JB et al (2015) Physiological role of taurine–from organism to organelle. Acta Physiol 213(1):191–212. https://doi.org/10.1111/apha.12365
41. Goodarzi A, Khanmohammadi M, Ebrahimi-Barough S et al (2019) Alginate-based hydrogel containing taurine-loaded chitosan nanoparticles in biomedical application. Arch Neurosci 6(2):e86349. https://doi.org/10.5812/ans.86349
42. Khorani M, Bobe G, Matthews DG et al (2022) The impact of the hAPP695^{SW} transgene and associated amyloid-β accumulation on murine hippocampal biochemical pathways. J Alzheimers Dis 85(4):1601–1619. https://doi.org/10.3233/Jad-215084
43. Khanmohammadi M, Sakai S, Taya M (2017) Impact of immobilizing of low molecular weight hyaluronic acid within gelatin-based hydrogel through enzymatic reaction on behavior of enclosed endothelial cells. Int J Biol Macromol 97:308–316. https://doi.org/10.1016/j.ijbiomac.2016.12.088
44. Wu L, Zhang QW, Li Y et al (2021) Collagen sponge prolongs taurine release for improved wound healing through inflammation inhibition and proliferation stimulation. Ann Transl Med 9(12):1010. https://doi.org/10.21037/atm-21-2739
45. Comino-Sanz IM, Lopez-Franco MD, Castro B et al (2021) The role of antioxidants on wound healing: a review of the current evidence. J Clin Med 10(16):3558. https://doi.org/10.3390/jcm10163558
46. Baek YY, Cho DH, Choe J et al (2012) Extracellular taurine induces angiogenesis by activating ERK-, Akt-, and FAK-dependent signal pathways. Eur J Pharmacol 674(2–3):188–199. https://doi.org/10.1016/j.ejphar.2011.11.022
47. Khoshfetrat AB, Khanmohammadi M, Sakai S et al (2016) Enzymatically-gellable galactosylated chitosan: hydrogel characteristics and hepatic cell behavior. Int J Biol Macromol 92:892–899. https://doi.org/10.1016/j.ijbiomac.2016.08.003
48. Khanmohammadi M, Sakai S, Ashida T et al (2016) Production of hyaluronic-acid-based cell-enclosing microparticles and microcapsules via enzymatic reaction using a microfluidic system. J Appl Polym Sci 133(16):43107. https://doi.org/10.1002/app.43107
49. Firouzi N, Khoshfetrat AB, Kazemi D (2020) Enzymatically gellable gelatin improves nano-hydroxyapatite-alginate microcapsule characteristics for modular bone tissue formation. J Biomed Mater Res A 108(2):340–350. https://doi.org/10.1002/jbm.a.36820
50. Wu M, Du Y, Liu YW et al (2014) Low molecular weight hyaluronan induces lymphangiogenesis through LYVE-1-mediated signaling pathways. PLoS ONE 9(3):e92857. https://doi.org/10.1371/journal.pone.0092857
51. Karimifard S, Rezaei N, Jamshidifar E et al (2022) pH-responsive chitosan-adorned niosome nanocarriers for co-delivery of drugs for breast cancer therapy. ACS Appl Nano Mater 5(7):8811–8825. https://doi.org/10.1021/acsanm.2c00861
52. Vernon RB, Sage EH (1999) A novel, quantitative model for study of endothelial cell migration and sprout formation within three-dimensional collagen matrices. Microvasc Res 57(2):118–133. https://doi.org/10.1006/mvre.1998.2122
53. Yang XM, Sarvestani SK, Moeinzadeh S et al (2013) Effect of CD44 binding peptide conjugated to an engineered inert matrix on maintenance of breast cancer stem cells and tumorsphere formation. PLoS ONE 8(3):e59147. https://doi.org/10.1371/journal.pone.0059147
54. Reno C, Marchuk L, Sciore P et al (1997) Rapid isolation of total RNA from small samples of hypocellular, dense connective tissues. Biotechniques 22(6):1082. https://doi.org/10.2144/97226bm16
55. Guo R, Xu SJ, Ma L et al (2011) The healing of full-thickness burns treated by using plasmid DNA encoding VEGF-165 activated collagen–chitosan dermal equivalents. Biomaterials 32(4):1019–1031. https://doi.org/10.1016/j.biomaterials.2010.08.087
56. Badali E, Goodarzi A, Khodayari H et al (2022) Layered dermal reconstitution through epigallocatechin 3-gallate loaded chitosan nanoparticle within enzymatically crosslinked polyvinyl alcohol/collagen fibrous mat. J Biomater Appl 37(3):502–516. https://doi.org/10.1177/08853282221104175
57. Salehi M, Zamiri S, Samadian H et al (2021) Chitosan hydrogel loaded with *Aloe vera* gel and tetrasodium ethylenediaminetetraacetic acid (EDTA) as the wound healing material: in vitro and in vivo study. J Appl Polym Sci 138(16):e50225. https://doi.org/10.1002/app.50225
58. Pardue EL, Ibrahim S, Ramamurthi A (2008) Role of hyaluronan in angiogenesis and its utility to angiogenic tissue engineering. Organogenesis 4(4):203–214. https://doi.org/10.4161/org.4.4.6926
59. Chen WS, He SP, Xiang DM (2021) Hypoxia-induced retinal pigment epithelium cell-derived bFGF promotes the migration and angiogenesis of HUVECs through regulating TGF-β1/smad2/3 pathway. Cancer Lett 328(1):18–26. https://doi.org/10.1016/j.gene.2021.145695
60. Fagiani E, Christofori G (2013) Angiopoietins in angiogenesis. Cancer Lett 328(1):18–26. https://doi.org/10.1016/j.canlet.2012.08.018
61. Napoli S, Scuderi C, Gattuso G et al (2020) Functional roles of matrix metalloproteinases and their inhibitors in melanoma. Cells 9(5):1511. https://doi.org/10.3390/cells9051151
62. Kandhwal M, Behl T, Singh S et al (2022) Role of matrix metalloproteinase in wound healing. Am J Transl Res 14(7):4391–4405
63. Tampa M, Georgescu SR, Mitran MI et al (2021) Current perspectives on the role of matrix metalloproteinases in the pathogenesis of basal cell carcinoma. Biomolecules 11(6):903. https://doi.org/10.3390/biom11060903